REVIEW

Rheological behavior of 10W40 base oil containing different combinations of MWCNT-Al$_2$O$_3$ nanoparticles and determination of the target nano-lubricant for industrial applications

Mohammad Hemmat Esfe[1,3], Soheyl Alidoust[2,3], Hossein Hatami[4] and Davood Toghraie[5*]

Abstract

The main goal of this research is to compare the rheological behavior of hybrid nano lubricants (HNLs) with different composition ratios in a base oil. The purpose of the comparison is to determine the HNL with the best lubrication performance at the start of the vehicle. Theoretical methods have confirmed the non-Newtonian behavior in different laboratory conditions. HNLs with the composition ratio of 30:70 and 25:75 had the highest percentage of increase and decrease in viscosity, respectively 34.97% and -1.85% at T$=55$ °C, shear rate SR$=6665$ s^{-1} and solid volume fraction SVF$=1\%$ and T$=5$ °C, SR$=3999$ s^{-1} and SVF$=0.05\%$. To predict the viscosity of the desired HNL, in the RSM, a special model with an accuracy of R$^2=0.9997$ has been used. The margin of deviation (MOD) is determined in the range of $-3.43\% <$ MOD $< 4.75\%$. Viscosity sensitivity analysis shows that the greatest sensitivity will result from SVF changes at high SVFs. The experimental results of this study will introduce the optimal nano polishing to the craftsmen, and the theoretical part of this study will save the researchers from spending time and excessive economic costs.

Keywords Hybrid nano-lubricant (HNL), MWCNT, Comparative study, Rheological behavior, Response surface methodology (RSM)

Introduction

Nanotechnology refers to the science of using nano in the field of various sciences and techniques, which is widely used in many branches of science today, and researchers are seriously researching it [1–7]. Today, nanofluids (NFs) have shown an important role in the development of industry and technological progress in various fields of industry. The idea of using nanoparticles was proposed for the first time in 1904 by Maxwell [8] and an important evolution occurred in the field of fluid heat transfer. Murshed et al. [9] first introduced this suspended particle–fluid mixture as NF, then Choi [10] developed this concept widely. Conventional fluids have focused researchers' attention on NFs due to their performance and properties with lower thermophysical properties than the new class of smart fluids. The distribution of nanoparticles (NPs) in the base fluid due to the high thermal conductivity (TC) and also the change in mass transfer improves the thermophysical properties such as density,

*Correspondence:
Davood Toghraie
Toghraee@iaukhsh.ac.ir
[1] Department of Mechanical Engineering, Imam Hossein University, Tehran, Iran
[2] School of Chemistry, Damghan University, Damghan, Iran
[3] Nanofluid Advanced Research Team, Tehran, Iran
[4] Department of Mechanical Engineering, Lorestan University, Khorramabad, Iran
[5] Department of Mechanical Engineering, Khomeinishahr Branch, Islamic Azad University, Khomeinishahr, Iran

viscosity, and TC [11–14]. Viscosity is one of the most efficient thermophysical properties of lubricants, and the study of rheological properties of lubricants has been one of the most attractive topics for researchers [15–23]. Oils are used as a coolant and lubricant in various industrial systems to reduce friction between parts and their wear. They have various other uses, some of which are shown in Fig. 1. In a study, the effect of the addition of Al_2O_3-Fe_2O_3 NPs on the thermal properties of 10W40 engine oil was studied [24]. In this study, the effect of SVF (0, 0.25, 0.5, 1, 2 and 4%) was investigated. The experiments were performed in the temperature range of 25–65 °C. The results show that even the lowest TC (at SVF = 4%, about 33% improved the TC) of the NF. The percentage of this increase depends on various factors including the SVF, NP properties, base fluid properties, and temperature. NFs have found many applications due to their properties, which has made the study of these properties of particular importance. Also, because these properties depend on the SVF, the properties of the NF can be adjusted by changing the SVF. In 2003, the results of an experimental study of a cooling system report an increase in the cooling rate in the cooling system [25]. In another study, Wu et al. [26] investigated the potential of water/aluminum oxide NFs in cooling systems. Their results indicate an increase in the freezing rate of NFs. By adding 2% alumina NPs to the water, they reduced the solidification time by about 20.5% and increase the efficiency of the system. The results of research in this field indicate the improvement of the performance of cooling systems using NFs. Compared to the frequency of research in the field of TC, less research was done in the field of dynamic viscosity of NFs. A research team of Iranian experts tried to evaluate a wide range of behavioral issues of viscosity with changes in the factors of composition ratio, base fluid (oil/water/ethylene glycol, etc.), and the diversity of NPs [27–34]. In a study by Hemmat et al. [30], the rheological

Fig. 1 Applications of NF in various industries

behavior of Al_2O_3-MWCNT (65%-35%)/5W50 HNLs was evaluated to facilitate its applications in the automotive industry. Dynamic viscosity of HNLs was measured in SVF = 0 to 1% at temperatures between 5 and 55 °C and SR between SR = 666.5 to 10,664 s^{-1}. Their findings distinguish the behavior of the HNLs from the non-Newtonian type. It was also observed that with increasing SVF, the non-Newtonian behavior of HNLs was intensified. Conversely, increasing the temperature had the opposite effect. They also presented a new correlation based on temperature and SVF with a correlation accuracy of 0.9923 to predict the viscosity of HNLs. In a study in 2021 [35], the researchers experimentally investigated the rheological behavior of MWCNT-TiO_2 nanoparticles mixed in 5W40 base oil. They showed that the rheological behavior of base oil and HNL correspond to the classification of Newtonian and non-Newtonian fluids. The viscosity of HNL also increases with decreasing SR and temperature and increasing SVF, and the presence of NPs enhances the viscosity of the HNL by up to 790%. In 2019 [36], the viscosity behavior of MWCNT-Al_2O_3 (30:70)/5W50 HNL in the temperature range of 5–55 °C, SVF = 0.05 to 1%, and SR range of 666.5–11,997 s^{-1} were investigated. Viscosity measurements show pseudo-plastic behavior at all temperatures and SVFs. The results show that the viscosity of HNL decreases with increasing temperature and increases with increasing SVF. In addition, this study proposes an optimized NP ratio as an oil additive to eliminate the unwanted viscosity reduction after the addition of NPs for thermal recovery purposes. A group of Chinese researchers conducted various studies using the properties of nanofluids in their new and practical studies. They improved the performance of the heat exchanger by introducing a new heat exchange medium and reinforcing structure [37–39]. In another study, they addressed the issue of thermal management of electronic components based on structures and nanofluids inspired by the new wave [40], also the effect of bionic channel structure and nanofluids on the characteristics of electricity generation of waste heat utilization equipment has been the title of another study of this group [41]. What is investigated in this article is to focus on the comparative analysis of the rheological behavior of HNLs to select the optimal HNL. The target NFs in this study have different composition ratios of NP but the same base fluid. The effect of the ratio of different compounds on the behavior of viscosity and improvement of the desired nanofluid was compared with each other. By using different theoretical methods, the classification of flow type was determined. Finally, using RSM, an empirical model was presented to predict viscosity data with acceptable accuracy (validated using R-Squared and MOD). At the end of the analysis, the viscosity sensitivity was plotted for six different SVFs. The
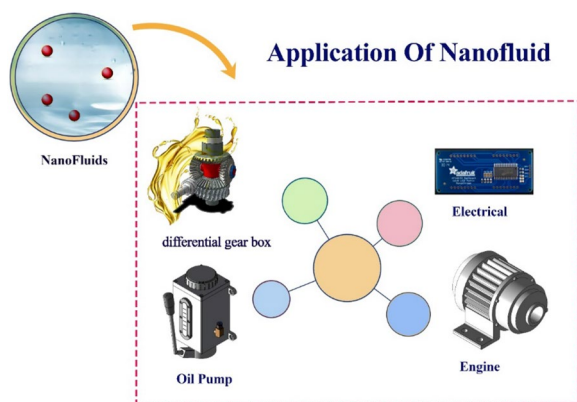
Fig. 2 NPs used in this study

results of this study, which is the result of a detailed and comprehensive comparison of the rheology and viscosity properties of the desired nanofluid, will introduce the optimal nanofluid to industrialists. Also, studying with the RSM method will save researchers from spending exorbitant laboratory costs in the future.

Experimental

Preparation of HNLs

HNLs require NPs and base oil. For this purpose, Al_2O_3 and MWCNT NPs and 10W40 base oil were used to make HNLs with different ratios of 25:75 and 30:70

(Fig. 2). The physical properties and strength properties of NPs are described in Table 1.

To determine the morphology (size and shape of NPs), surface properties (surface details of NPs), the crystal structure of NPs as well as NP identification, advanced scanning electron microscope (SEM) and transmission electron microscope (TEM) imaging methods and X-ray diffraction analysis (XRD) were used. The details are taken in Figs. 3, 4 and 5 with high magnification and accuracy.

Equation 1 was used to determine the amount of required nanomaterials in the preparation of HNLs with

Table 1 Specifications of MWCNT and Al_2O_3 NPs

NPs	Purity	APS	SSA	Color	True density	Morphology
MWCNT	> 95 wt%	5–15 nm	233 m^2/g	Black	~ 2.1 g/cm^3	Cylindrical
Al_2O_3	≥ 99%	20 nm	138 m^2/g	white	3.97 g/cm^3	Nearly spherical

Fig. 3 TEM pictures of used NPs

Hemmat Esfe *et al. Micro and Nano Systems Letters* (2023) 11:14

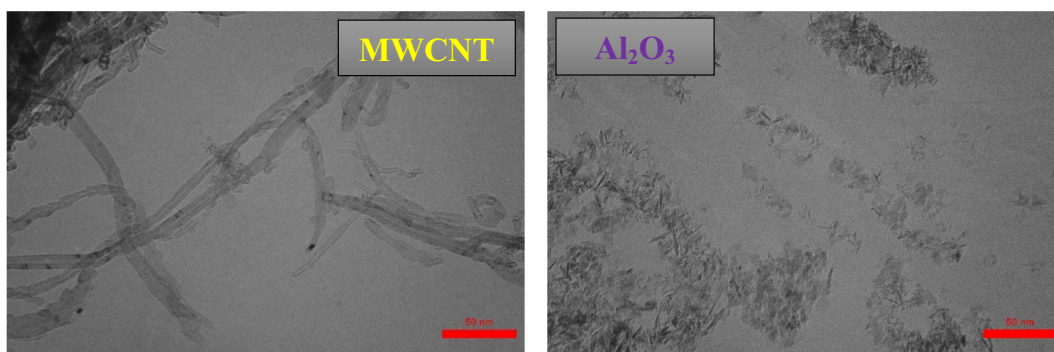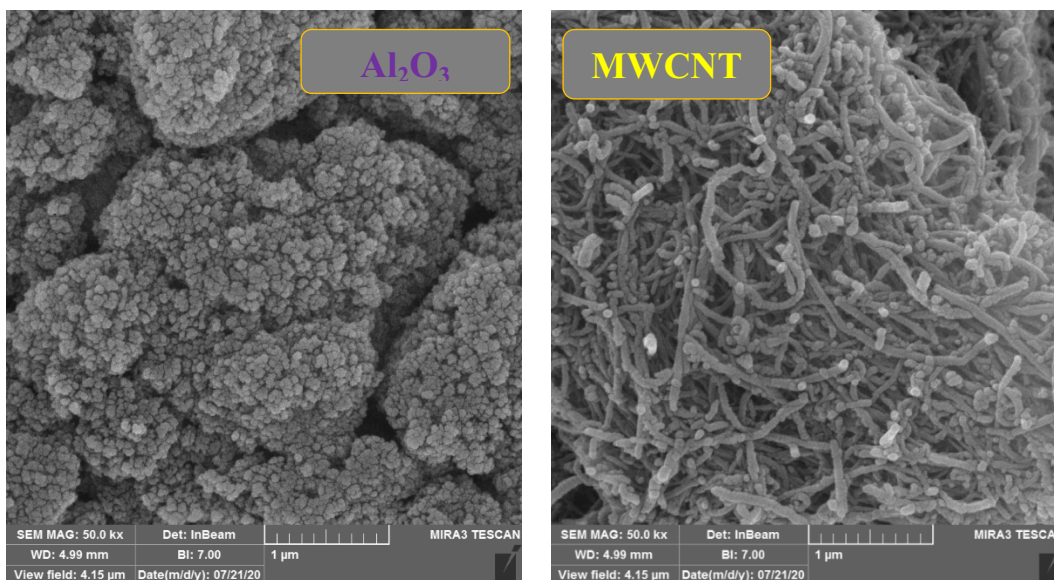Page 4 of 15

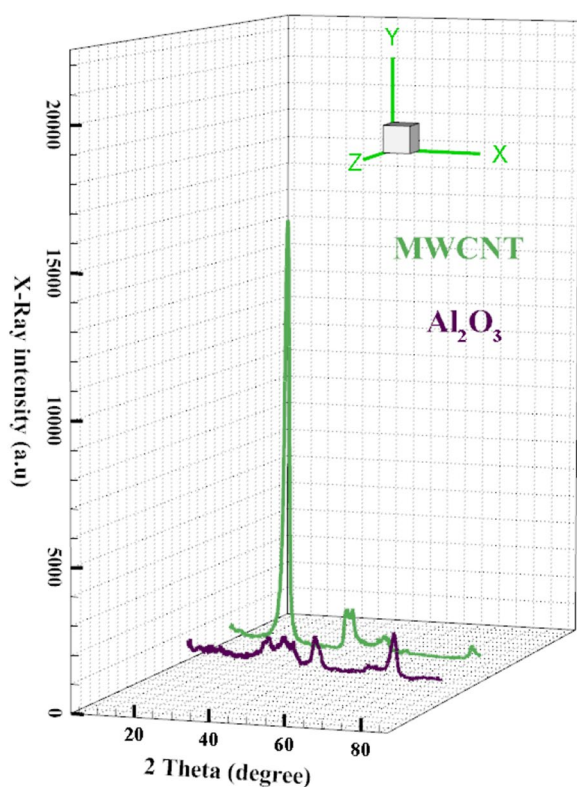
Fig. 4 SEM pictures of used NPs

Fig. 5 XRD analysis for used NPs

different SVFs. Also, for weighing nanomaterials, a digital scale with an accuracy of 0.001 gr was used.

$$SVF = \left(\frac{0.75\left(\frac{w}{\rho}\right)_{Al2O3} + 0.25\left(\frac{w}{\rho}\right)_{MWCNT}}{0.25\left(\frac{w}{\rho}\right)_{MWCNT} + 0.75\left(\frac{w}{\rho}\right)_{Al2O3} + \left(\frac{w}{\rho}\right)_{10W40} +} \right) \times 100 \tag{1}$$

A magnetic stirrer is required to mix the weighed NPs in the base fluid. This device was used for 1 h for the initial uniformity of the HNLs. Then, to increase the stability and break the NP clusters and prevent the formation of sediment, an ultrasonic vibrator was used for 1 h). As a result, it was observed that the prepared NFs in different SVFs were stable after three weeks. Figure 6 shows images of stabilized HNLs for different SVFs.

Measurement of dynamic viscosity

One way to obtain information about the rheological behavior of NFs is to use a Brookfield viscometer. The viscometer is used to determine the viscosity of fluids. Technical specifications and operating environment conditions are stated in Table 2. Prior to measurement, a calibration test was performed to prevent measurement errors. The range of conditions for measuring
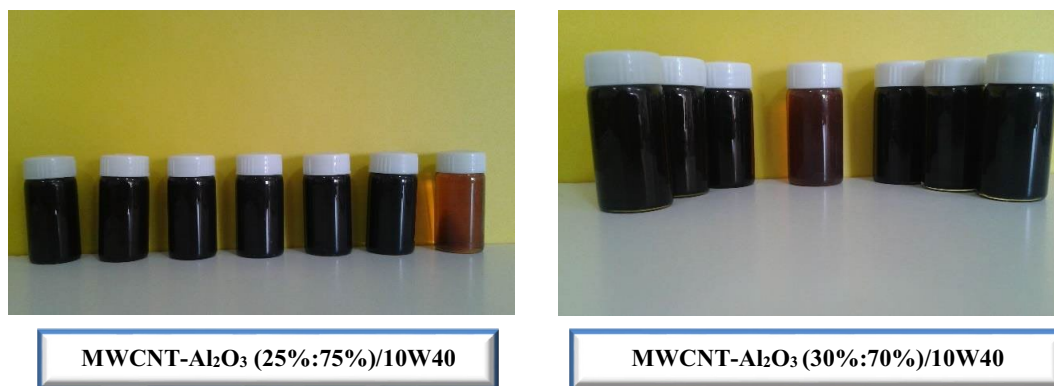
MWCNT-Al₂O₃ (25%:75%)/10W40   **MWCNT-Al₂O₃ (30%:70%)/10W40**

Fig. 6 HNL samples prepared at different SVFs

Table 2 Viscometer technical specifications

Specification	CAP 2000+
Inlet Voltage	115–230 V
Inlet Frequency	50–60 Hz
Power consumption	Less than 345 V
Torque range	18,100 rpm
Speed	5–1000 rpm
Temperature	5–55 °C
Material	Conical spindles and thermal plates are made from tungsten carbide and the sample holder is made from Teflon
Impact of environmental factors	CAP 2000 + Viscometer needs to work in the below conditions: Environmental temperature: 5–20 °C Humidity: 20–80%

Table 3 Laboratory conditions for measuring HNL viscosity

HNL	Range of laboratory condition		
	T (°C)	SVF (%)	SR (s^{-1})
MWCNT/ Al₂O₃(25%:75%)-10W40	5–55	0.05–1	666.5–11,997
MWCNT/ Al₂O₃(30%:70%)-10W40	5–55	0.05–1	666.5–11,997

the viscosity of HNLs is shown in Table 3. To reduce the effect of viscometer measurement error, all experiments were measured twice and then the average data were recorded. Some of the measured viscosity data are reported in Table 4.

Table 4 Some results measured with CAP2000 + viscometer

HNL	SVF (%)	T (°C)	SR (s^{-1})	μ(mPa.s)
MWCNT/ Al₂O₃(25%:75%)- 10W40	0.05	5	666.5	551
	0.1	15	1333	294
	0.25	25	3999	160.6
	0.5	35	6665	96
	0.75	45	9331	62.4
	1	55	10,664	45
MWCNT/ Al₂O₃(30%:70%)- 10W40	0.05	5	666.5	566
	0.1	15	1333	300
	0.25	25	3999	161.9
	0.5	35	6665	98.6
	0.75	45	9331	64.6
	1	55	10,664	47.3

Comparison and discussion
Rheological behavior
Shear stress-SR
One of the methods to evaluate the rheological behavior of HNLs is to investigate the shear stress at different SRs. In general, the slope of these curves is equal to the viscosity of HNLs. In the curves of Fig. 7, the shear stress versus the SR for two similar HNLs with the same base fluid with different percentages in the lowest and
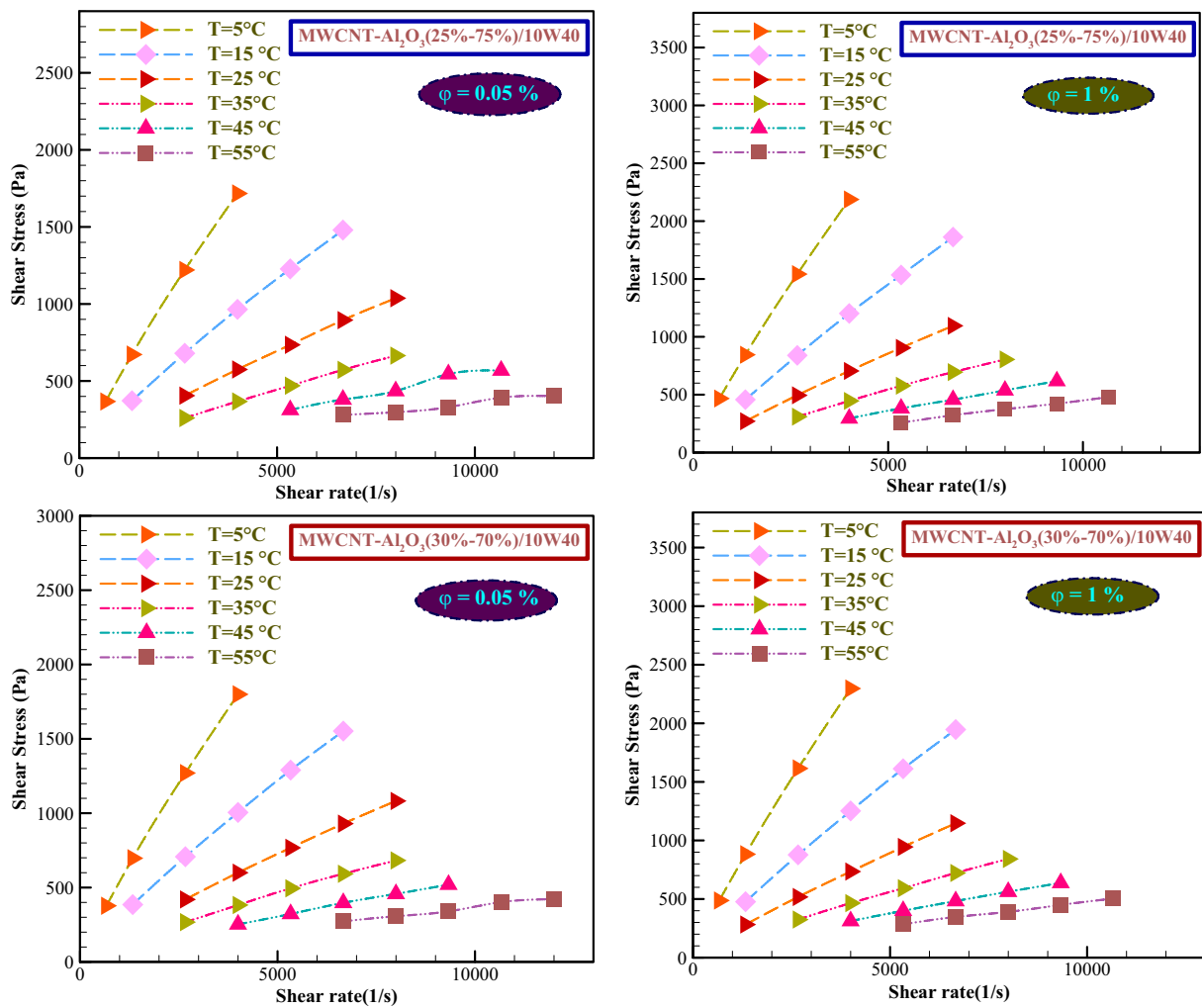
Fig. 7 Curve of changes in shear stress-SR at different laboratory conditions

highest SVFs is shown. According to Eq. 2, for Newtonian fluid, there is a linear relationship between SR and shear stress. In the case of fluids with non-Newtonian behavior, the shear stress is a nonlinear function of the SR. According to the curves of Fig. 7, the behavior of HNLs in different temperatures and SVFs will be non-Newtonian.

$$\tau = \mu * SR \tag{2}$$

Power-law index

To ensure the non-Newtonian behavior of HNLs, the power-law model method was used. For this purpose, the power-law index curves according to Eq. 3, are plotted in Fig. 8 for both HNLs relative to temperature in different SVFs.

$$\tau = m * SR^n \tag{3}$$

According to Fig. 8, both HNLs can be classified as non-Newtonian fluids because they are lower than the index line with a certainty of n values in all SVFs. However, more precisely in Table 4, the values of n in several SVFs and at all studied temperatures are reported. Table 5 shows that at T = 55 °C, the behavior of these HNLs tends to be non-Newtonian fluids even more than other temperatures. As a result, HNLs can show a suitable reaction to enhance lubrication in different engine operating conditions.

To make a more accurate and statistical comparison of the behavior of the two HNLs under comparison, the results of the power-law index values are reported in Table 5. The results show that both HNLs have a value of n less than 1 at all temperatures. MWCNT-Al_2O_3 (25–75%)/10W40 HNL at T = 55 °C and SVF = 0.05% shows

Hemmat Esfe *et al. Micro and Nano Systems Letters* (2023) 11:14
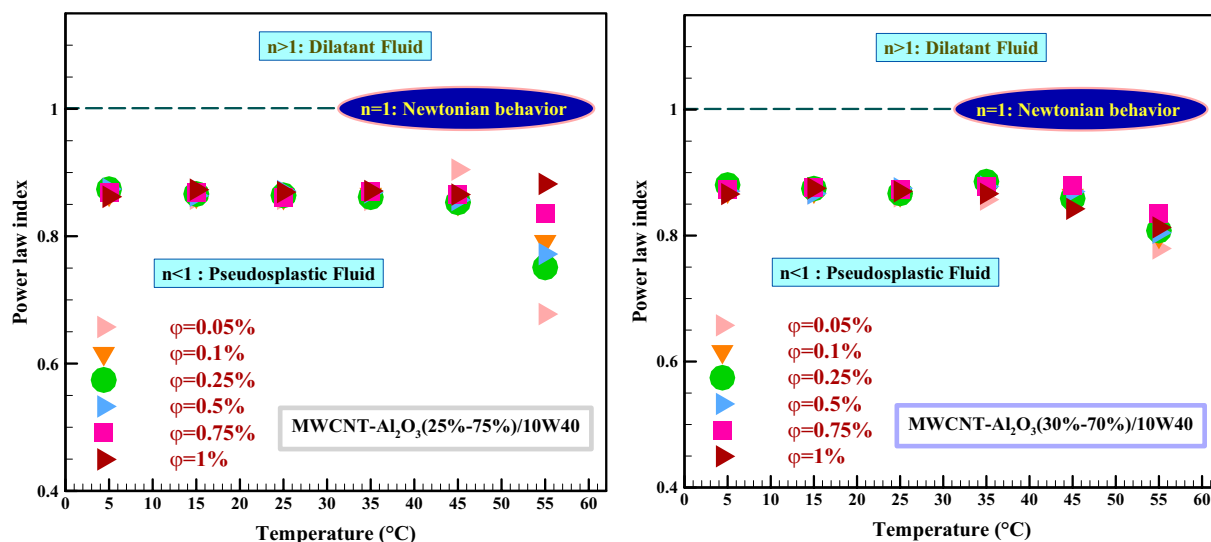
Page 7 of 15

Fig. 8 Effect of main parameters (temperature and SVF) on power-law index

Table 5 Power law index values at different laboratory conditions

HNF		Power-law index (n)					
		T = 5 °C	T = 15 °C	T = 25 °C	T = 35 °C	T = 45 °C	T = 55 °C
MWCNT-Al_2O_3 (25–75%)/10W40	SVF	0.8615	0.8588	0.8587	0.8571	0.9046	0.6777
	SVF	0.866	0.8628	0.8609	0.8658	0.8515	0.7917
	SVF	0.8738	0.8663	0.8642	0.8615	0.8532	0.7511
	SVF	0.8741	0.8636	0.8709	0.8689	0.8569	0.772
	SVF	0.8684	0.8693	0.8611	0.8706	0.8649	0.8357
	SVF	0.8621	0.8731	0.8694	0.871	0.8654	0.8821
MWCNT-Al_2O_3 (30–70%)/10W40	SVF	0.8717	0.8675	0.8622	0.8571	0.8564	0.7795
	SVF	0.8705	0.8705	0.8647	0.8748	0.864	0.7986
	SVF	0.8804	0.8746	0.8669	0.8858	0.859	0.8079
	SVF	0.8703	0.8667	0.8752	0.8778	0.8699	0.8044
	SVF	0.8726	0.8769	0.8731	0.8773	0.8801	0.8355
	SVF	0.8659	0.8751	0.8702	0.8665	0.8425	0.813

stronger non-Newtonian behavior. On the other hand, both HNLs are more prone to non-Newtonian behavior at higher temperatures and SVFs.

Viscosity-SR
Investigating the effect of SR on viscosity can be introduced as the next method to describe the rheological behavior of HNLs. In Fig. 9 as an example, the viscosity curve in terms of SR in the temperature range of T = 5–55 °C and SVF = 0.05% for the MWCNT-Al_2O_3 (25–75%) /10W40 and MWCNT-Al_2O_3 (30–70%)/10W40 HNLs was compared versus the 10W40 base fluid. According to the obvious principles in fluid mechanics, the dependence of the viscosity on SR indicates that the behavior of the HNL is close to that of the non-Newtonian fluid. Therefore, the dependence of the viscosity of HNLs on SR in Fig. 9 indicates that the HNLs are non-Newtonian. Also, for more reliability and observation of changes in viscosity, magnification was done at T = 5 °C and 55 °C. As can be seen, the viscosity was decreased with respect to the temperature with a significant slope. Of course, the slope of changes at low temperatures is greater.
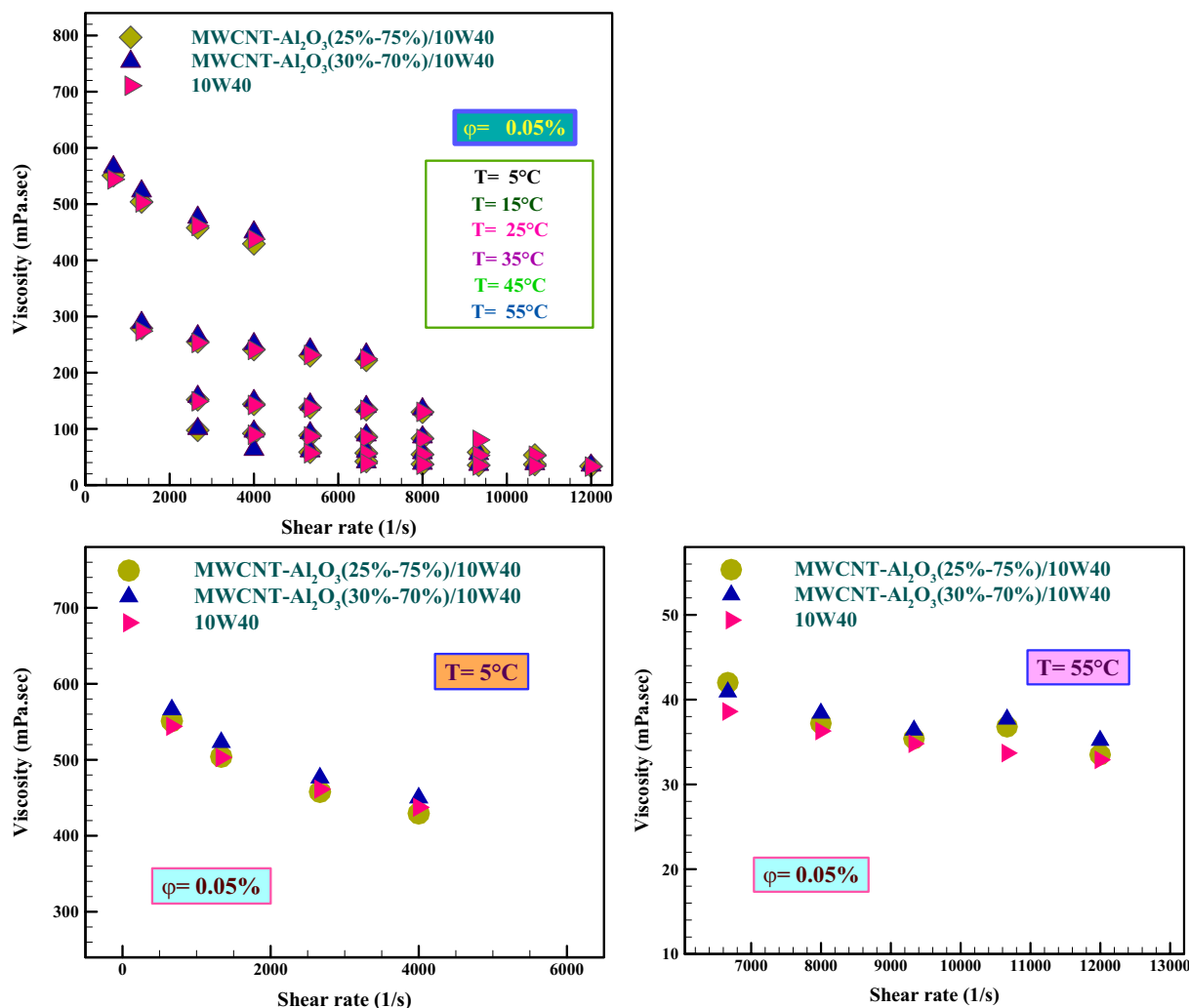
Fig. 9 Viscosity-SR at different laboratory conditions

Viscosity comparison

Viscosity enhancement

After investigating the rheological behavior of HNLs, the viscosity of HNLs was compared. The curves shown in Figs. 10 and 11 show the changes in viscosity enhancement to SVF for HNLs at SR = 3999 and 6665 s^{-1} and different temperatures. According to Eq. 4, viscosity enhancement is obtained from the difference between the viscosity of the HNL and the base fluid divided by the base fluid, which is reported as a percentage.

$$\text{Viscosity enhancement (\%)} = \frac{\mu_{nf} - \mu_{bf}}{\mu_{bf}} \times 100 \quad (4)$$

According to Table 6, the maximum viscosity reduction belonged to MWCNT-Al$_2$O$_3$ (25–75%)/10W40 HNL in SVF = 0.05% and T = 5 °C, which is equal to −1.85%. On the other hand, the maximum increase in viscosity

at T = 55 °C and SVF = 1% belonged to MWCNT-Al$_2$O$_3$ (30%-70%) / 10W40 HNL and was equal to 34.97%.

Figure 12 schematically shows the rheological performance of the studied HNLs in the present study in industrial applications.

The effect of temperature on viscosity

After dispersion NPs into the oil, the viscosity was calculated at all temperatures and quantitatively reported in SVF = 0.05% in Table 7. Figure 13 compares the viscosity-temperature curves at SVF = 0.05% and SR = 3999 and 6665 s^{-1}. According to the results, the addition of MWCNT and Al$_2$O$_3$ NPs with the ratio of (25:75) only at T = 5 °C reduces the viscosity of HNLs by −1.85%. In this sense, this HNL can be considered by craftsmen.

Figure 14 and Table 8 compare and analyze the viscosity results of HNLs in SVF = 0.1%. Unfortunately,
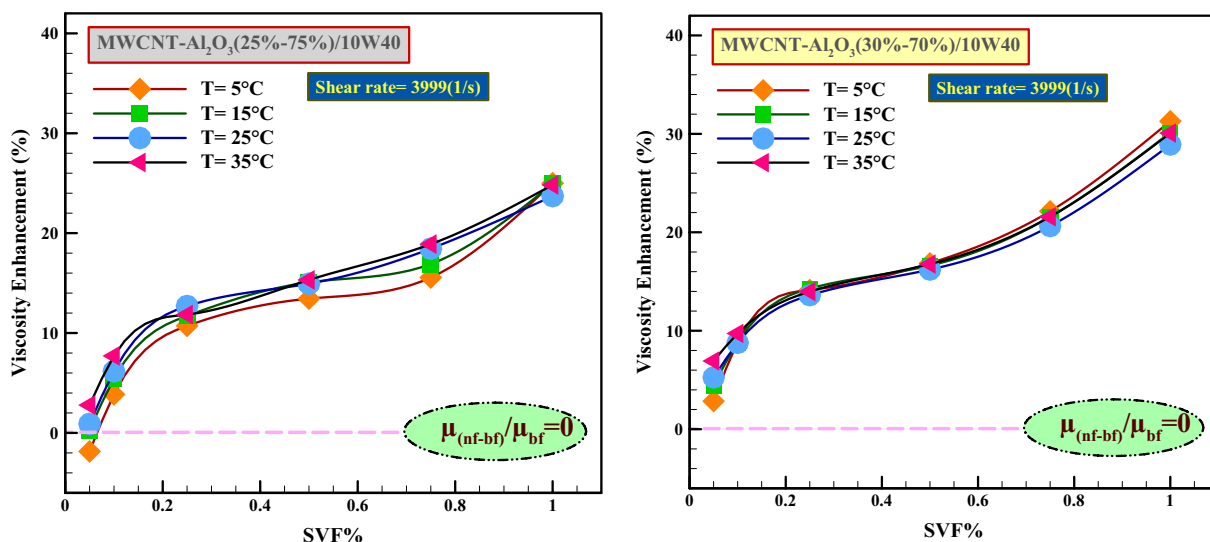
Fig. 10 Relative viscosity in terms of SVF at different temperatures at SR = 3999 s^{-1}
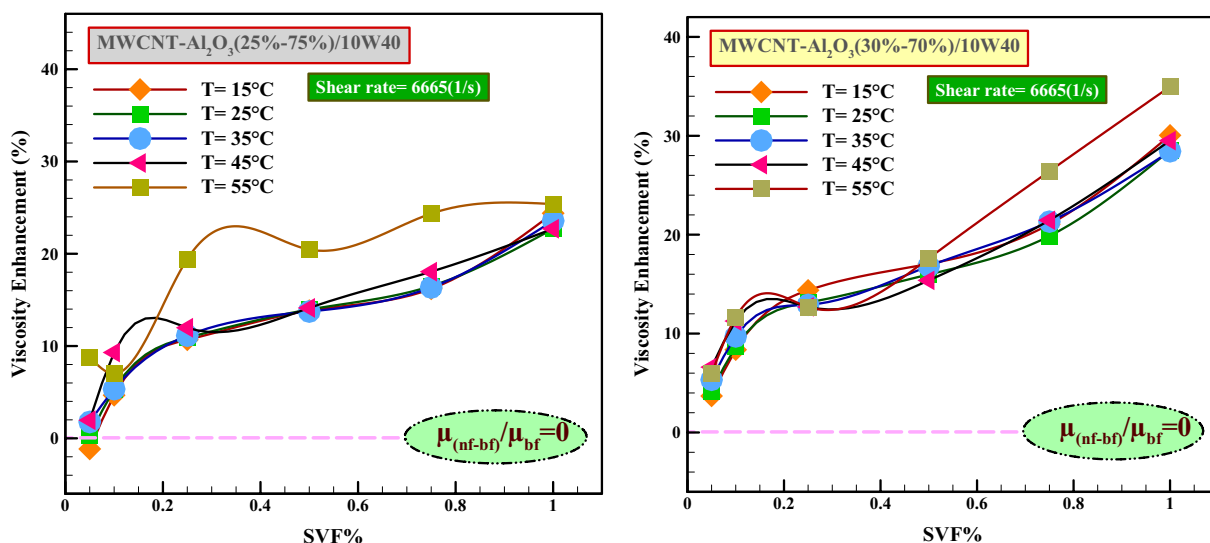

Fig. 11 Relative viscosity in terms of SVF at different temperatures at SR = 6665 s^{-1}

at SVF = 0.1%, at no temperature, the desired viscosity behavior was not observed for any of the HNLs.

Impractical results

RSM method

The purpose of using the RSM in this study is to determine the relationship between the target response and the variables affecting it in the form of providing a predictive relationship as well as modeling experimental data. For this purpose, laboratory data were normalized with the Quartic model due to statistical inadequacy and then the results were extracted. Laboratory data including temperature, SR and SVF were introduced as input

and viscosity data (target response) as output to Design of expert (DOE) software. Tables 9 and 10 show the statistical outputs of the normalized data using the quadratic model.

New correlation

To predict the experimental data of the selected HNL as well as how the interaction between the target response and the independent variables, a nonlinear three-variable-quadratic relationship was used. The condition for using Eq. 5 is to observe the range of test conditions, which is unacceptable outside this range.

Table 6 Statistical data on the percentage change of viscosity enhancement of HNLs

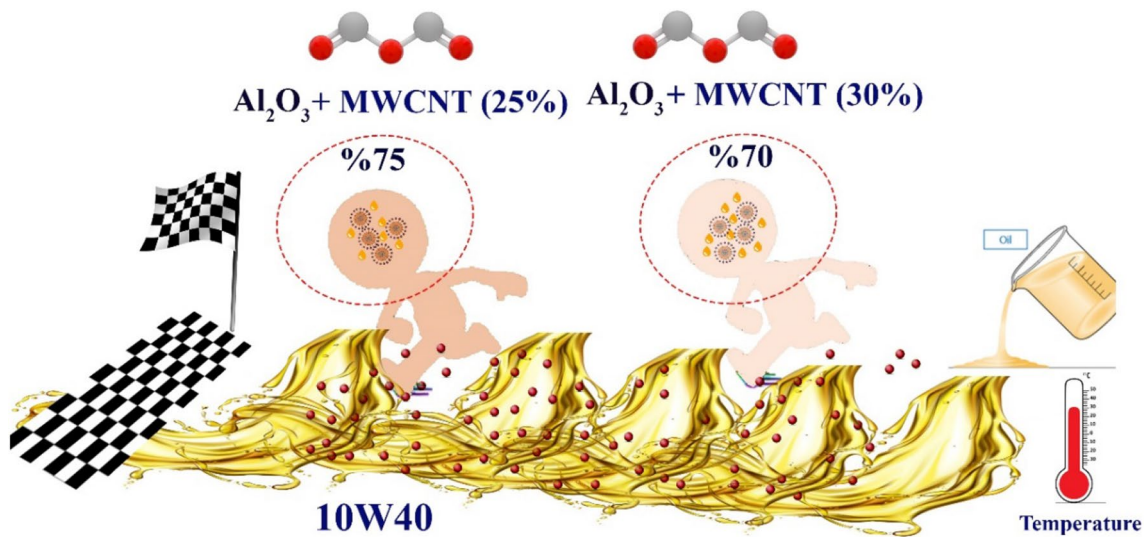| HNL	SR(s^{-1})	T (°C)	$\left(\frac{\mu_{nf}-\mu_{bf}}{\mu_{bf}}\right)$%			
			SVF = 0.05%	0.1%	0.75%	1%
MWCNT-Al$_2$O$_3$ (25–75%)/10W40	3999 (300 rpm)	5	−1.85	3.86	15.56	25
		15	0.29	5.44	16.91	24.93
		25	0.91	6.17	18.45	23.71
		35	2.79	7.71	18.90	24.83
	6665 (500 rpm)	15	−1.15	4.67	16.20	24.39
		25	0.29	5.30	16.50	22.70
		35	1.77	5.33	16.35	23.57
		45	1.96	9.30	18.06	22.71
		55	8.80	6.99	24.35	25.38
MWCNT-Al$_2$O$_3$ (30–70%)/10W40	3999 (300 rpm)	5	2.85	8.86	22.14	31.29
		15	4.44	8.85	21.57	30.13
		25	5.26	8.77	20.63	28.91
		35	6.93	9.73	21.58	30.08
	6665 (500 rpm)	15	3.69	8.37	21.05	30.05
		25	4.18	8.66	19.86	28.52
		35	5.33	9.71	21.32	28.43
		45	6.61	11.27	21.46	29.51
		55	5.95	11.65	26.42	34.97

Fig. 12 The rheological performance of studied HNLs in the present study in industrial applications

$$
\begin{aligned}
\left(\text{Viscosity}\right)^{0.55} = {} & +39.87127 - 1.45299\text{T} - 1.69500\text{E} - 003 + 7.37688\text{E} - 005\,\text{T}\dot{\gamma} \\
& + 0.030075\text{T}^2 + 18.30736 SVF^2 + 9.14611E - 004\,\text{T}^2 * SVF - 0.22282 TSVF^2 \\
& - 8.86737\text{E} - 009\,T^2 - 3.11056\text{E} - 010 SVF * \text{SR}^2 - 4.15818\text{E} - 004\text{T}^3 - 29.23742 SVF^3 \\
& + 2.28810\text{E} - 011^3 + 4.04801\text{E} - 011\,\text{T}^{2^2} + 0.12543\,\text{T} * SVF^3 + 2.22791\text{E} - 006\text{T}^4 + 14.64807^4 - 5.14218\text{E} - 016^4
\end{aligned}
\tag{5}
$$

Table 7 Comparative study of the effect of temperature on the viscosity of HNLs relative to the base fluid at SVF = 0.05%

SR (s^{-1})	T (°C)	$\Delta(\mu_{n-b})_f$ MWCNT-Al$_2$O$_3$ (25%-75%) /10W40	$\Delta(\mu_{n-b})_f$ MWCNT-Al$_2$O$_3$ (30%-70%)/10W40	T (°C)
3999	5	−8.1 (−1.85%)	12.5(2.85%)	5
	15	0.7	10.7	15
	25	1.3	7.5	25
	35	2.5	6.2	35
6665	35	1.5	4.5	35
	45	1.1	4.6	45
	55	3.4	2.3	55

In Fig. 15, the modeled data have an acceptable correlation with the experimental data on the criterion line.

Margin of deviation (MOD)

The standard MOD method is used to determine the degree of scattering and deviation of the data relative to the zero standard line. Equation 6 was used to calculate the MOD.

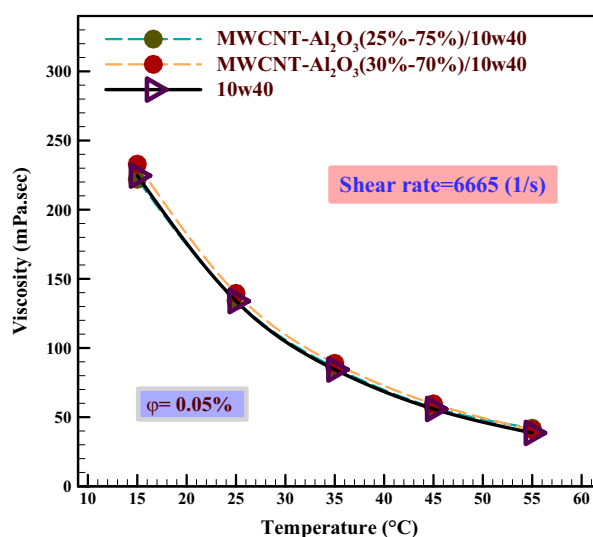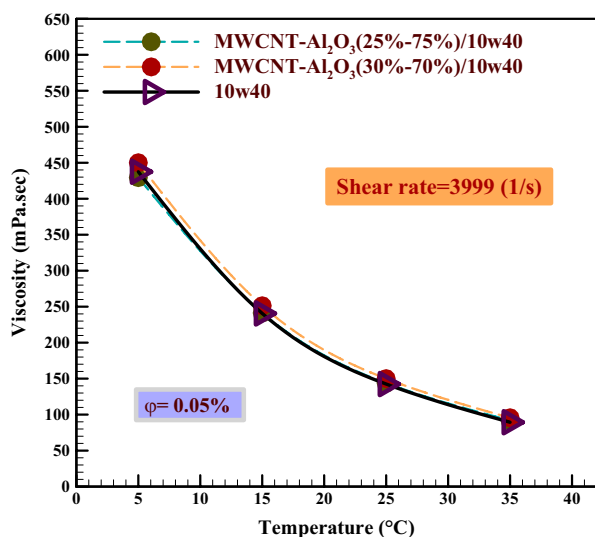$$MOD = \frac{\mu_{rel_{exp}} - \mu_{rel_{pre}}}{\mu_{rel_{exp}}} \times 100 \tag{6}$$

Fig. 13 Comparison of the effect of temperature on the viscosity of the studied HNLs in SVF = 0.05%
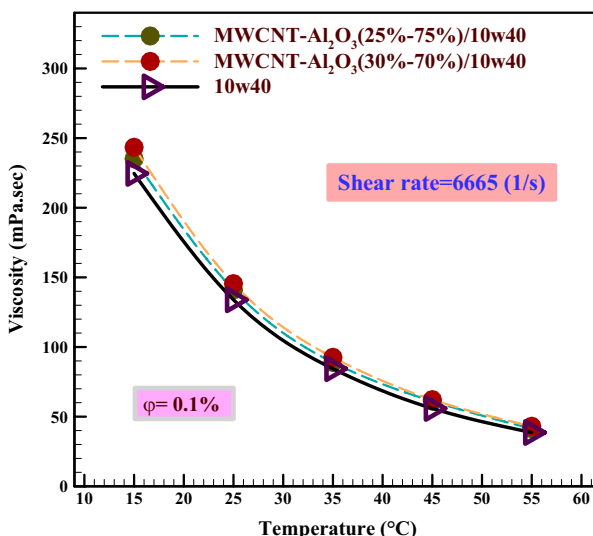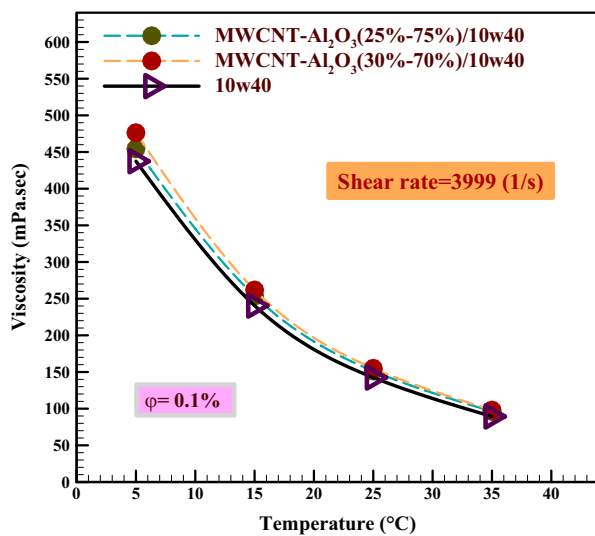

Fig. 14 Comparison of the effect of temperature on the viscosity of the studied HNLs in SVF = 0.1%

Table 8 Comparative study of the effect of temperature on the viscosity of HNLs relative to the base fluid at SVF = 0.1%

SR (s^{-1})	T (°C)	$\Delta(\mu_{n-b})_f$ MWCNT-Al$_2$O$_3$ (25%-75%)/10W40	$\Delta(\mu_{n-b})_f$ MWCNT-Al$_2$O$_3$ (30%-70%)/10W40	T (°C)
3999	5	16.9(3.86%)	38.8(8.86%)	5
	15	13.1	21.3	15
	25	8.8	12.5	25
	35	6.9	8.7	35
6665	35	4.5	8.2	35
	45	5.2	6.3	45
	55	2.7	4.5	55

Table 9 Optimized modeling accuracy

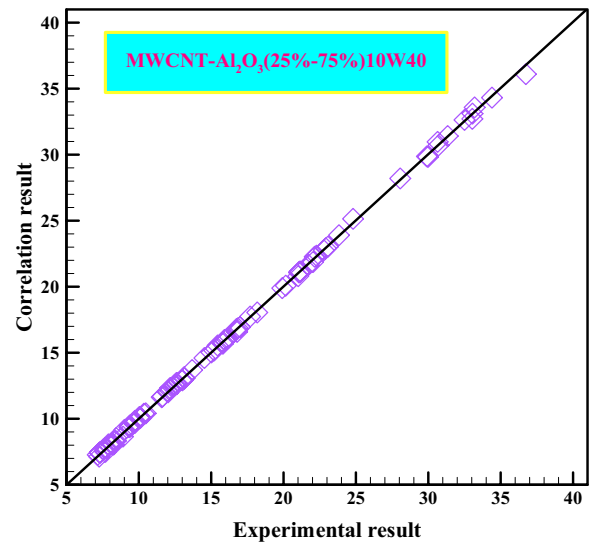| Std. Dev	0.14	R-Squared	0.9997
Mean	16.17	Adj R-Squared	0.9997
C.V. %	0.85	Pred R-Squared	0.9996
PRESS	4.05	Adeq Precision	658.162

Fig. 15 Correlation of predicted data with actual data

Table 10 ANOVA for Response surface quartic model

Source	Sum of squares	df	Mean square	F value	p-value Prob > F	
Model	10,913.38	17	641.96	34,257.29	< 0.0001	significant
A-T	460.77	1	460.77	24,588.31	< 0.0001	
C-Shear rate	3.50	1	3.50	186.72	< 0.0001	
AC	0.20	1	0.20	10.81	0.0012	
A^2	19.81	1	19.81	1057.19	< 0.0001	
B^2	0.12	1	0.12	6.17	0.0141	
A^{2}B	1.78	1	1.78	95.02	< 0.0001	
AB^2	0.085	1	0.085	4.55	0.0346	
AC^2	1.21	1	1.21	64.69	< 0.0001	
BC^2	0.095	1	0.095	5.05	0.0260	
A^3	19.53	1	19.53	1042.20	< 0.0001	
B^3	16.92	1	16.92	903.16	< 0.0001	
C^3	0.24	1	0.24	12.62	0.0005	
A^{2}C^2	0.82	1	0.82	43.83	< 0.0001	
AB^3	13.87	1	13.87	740.28	< 0.0001	
A^4	0.57	1	0.57	30.64	< 0.0001	
B^4	0.30	1	0.30	15.98	< 0.0001	
C^4	0.60	1	0.60	32.17	< 0.0001	
Residual	2.92	156	0.019			
Cor Total	10,916.30	173				

Transform: Power, Lambda: 0.55, Constant: 0
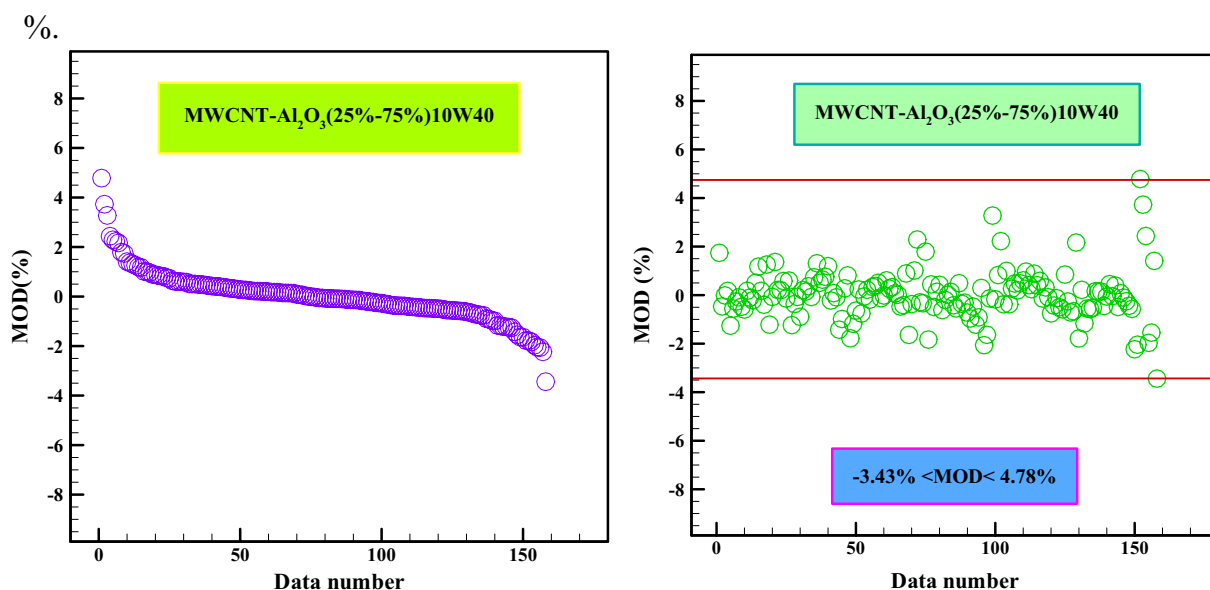
%.

Fig. 16 Range of MOD values in all laboratory data
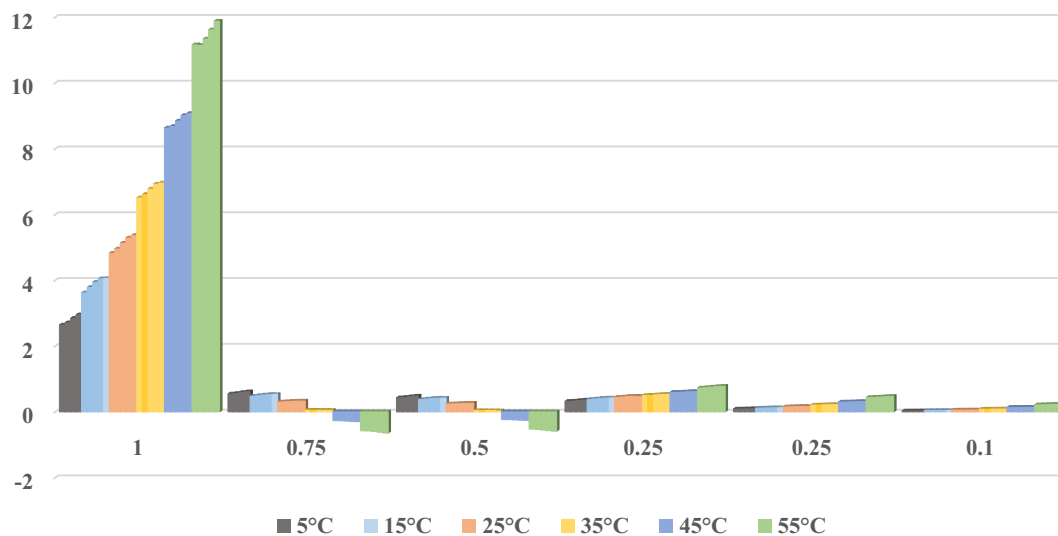
Viscosity Sensitivity Analysis

Fig. 17 Viscosity sensitivity analysis for all data in different laboratory conditions

Figure 16 shows the range of MOD values for all laboratory data. The allowable range of MOD values for the selected HNL was set at $-3.43\% < MOD < 4.75$.

Viscosity sensitivity

Sensitivity analysis is a method to determine the effect of different effective parameters on the target response. In this study, only the effect of SVF change on viscosity was investigated. Equation 7 was used to calculate the viscosity sensitivity to calculate.

$$Viscosity\ sensitivity$$
$$= \frac{\left(Viscosity_{after\ change}\right)_{Pre} - \left(Viscosity_{before\ change}\right)_{Pre}}{\left(Viscosity_{before\ change}\right)_{Pre}} \times 100$$

$$(7)$$

Hemmat Esfe *et al. Micro and Nano Systems Letters*   (2023) 11:14

Page 14 of 15

Figure 17 shows the viscosity sensitivity for 6 different SVFs with + 10% variations. Observations show that the highest sensitivity was occurred in high SVFs.

Conclusion

In this study, the rheological behavior of hybrid nano-lubricants (HNLs) is compared that differ in the ratio of components in the base oil. The purpose of the comparison is to determine the HNL with the best lubrication performance at the start of the vehicle. The results of this study are summarized in the following cases:

- Observing the pseudo-plastic non-Newtonian fluid.
- Observing more viscous HNLs with a composition ratio of 30:70 compared to HNLs with a composition ratio of 25:75 in equal conditions with an increase in SVF.
- Observing the decrease in viscosity in low SVFs due to the presence of NPs in the layers between the HNL and facilitating the sliding of the layers on top of each other.
- Optimal efficiency of the RSM in predicting viscosity values and constructing an experimental model
- Observing the greatest sensitivity to changes in high SVFs

Declarations

Ethics approval and consent to participate
N/A.

Consent for publication
N/A.

Competing interests
N/A.

References

1. Cui X, Li C, Yang M, Liu M, Gao T, Wang X, Said Z, Sharma S, Zhang Y (2023) Enhanced grindability and mechanism in the magnetic traction nanolubricant grinding of Ti-6Al-4V. Tribol Int 186:108603. https://doi.org/10.1016/j.triboint.2023.108603
2. Zhang X, Li C, Zhou Z, Liu B, Zhang Y, Yang M, Gao T, Liu M, Zhang N, Said Z, Sharma S, Muhammad Ali H (2023) Vegetable oil-based nanolubricants in machining: from physicochemical properties to application. Chin J Mech Eng 36:76. https://doi.org/10.1186/s10033-023-00895-5
3. Shekoofa O, Wang J, Li D (2023) Fabrication of n-type nanocrystalline silicon thin-film by magnetron sputtering and antimony induced crystallization. Arch Adv Eng Sci. https://doi.org/10.47852/bonviewAAES32021040
4. Alizadeh A, Jasim Mohammed K, Fadhil Smaisim G, Hadrawi SK, Zekri H, Taheri Andani H, Nasajpour-Esfahani N, Toghraie D (2023) Evaluation of the effects of the presence of ZnO -TiO2 (50 %–50 %) on the thermal conductivity of Ethylene Glycol base fluid and its estimation using Artificial Neural Network for industrial and commercial applications. J Saudi Chem Soc 27(2):101613. https://doi.org/10.1016/j.jscs.2023.101613
5. Dai X, Andani HT, Alizadeh A, Abed AM, Smaisim GF, Hadrawi SK, Karimi M, Shamsborhan M, Toghraie D (2023) Using Gaussian Process Regression (GPR) models with the Matérn covariance function to predict the dynamic viscosity and torque of SiO2/Ethylene glycol nanofluid: a machine learning approach. Eng Appl Artif Intell 122(106107):106107. https://doi.org/10.1016/j.engappai.2023.106107
6. Athab A, Lafta AJ, Hussein FH (2015) Modification of carbon nanotubes surface using different oxidizing agents. J Environ Anal Chem 2:e112
7. Ruhani B, Barnoon P, Toghraie D (2019) Statistical investigation for developing a new model for rheological behavior of Silica–ethylene glycol/Water hybrid Newtonian nanofluid using experimental data. Physica A 525:616–627
8. Maxwell JC (1873) A treatise on electricity and magnetism, vol 1. Clarendon press, Oxford
9. Murshed SMS, Leong KC, Yang C (2008) Investigations of thermal conductivity and viscosity of nanofluids. Int J Therm Sci 47(5):560–568
10. Choi SU, Eastman JA (1995) Enhancing thermal conductivity of fluids with nanoparticles (No. ANL/MSD/CP-84938; CONF-951135–29). Argonne National Lab.(ANL), Argonne, IL (United States)
11. Bozorg MV, Doranehgard MH, Hong K, Xiong Q (2020) CFD study of heat transfer and fluid flow in a parabolic trough solar receiver with internal annular porous structure and synthetic oil–Al2O3 nanofluid. Renew Energy 145:2598–2614
12. Hemmat Esfe M (2017) Designing an artificial neural network using radial basis function (RBF-ANN) to model thermal conductivity of ethylene glycol–water-based TiO2 nanofluids. J Therm Anal Calorim 127(3):2125–2131
13. Asadi A et al (2018) Heat transfer efficiency of Al2O3-MWCNT/thermal oil hybrid nanofluid as a cooling fluid in thermal and energy management applications: an experimental and theoretical investigation. Int J Heat Mass Transfer. 117:474–486
14. Alidoust S, Zamani M, Jabbari M (2020) Sol-gel synthesis of nanoporous γ-alumina using TX-100 or gelatin/TX-100 mixture as effective catalysts for dehydration of alcohols. Iran J Catal 10(4):295–305
15. Zhang G, Zhang Z, Sun M, Yu Y, Wang J, Cai S (2022) The influence of the temperature on the dynamic behaviors of magnetorheological gel. Adv Eng Mater. https://doi.org/10.1002/adem.202101680
16. Zhang G, Chen J, Zhang Z, Sun M, Yu Y, WangCai JS (2022) Analysis of magnetorheological clutch with double cup-shaped gap excited by Halbach array based on finite element method and experiment. Smart Mater Struct. https://doi.org/10.1088/1361-665X/ac701a
17. Putra ABW (2020) Computer technology simulation towards power generation potential from coproduced fluids in south Lokichar oil fields. Int J Commun Comput Technol 8(2):9–12. https://doi.org/10.31838/ijccts/08.02.03
18. Yang M, Li C, Zhang Y, Jia D, Zhang X, Hou Y, Li R, Wang J (2017) Maximum undeformed equivalent chip thickness for ductile-brittle transition of zirconia ceramics under different lubrication conditions. Int J Mach Tools Manuf 122:55–65. https://doi.org/10.1016/j.ijmachtools.2017.06.003
19. Gao T, Li C, Zhang Y, Yang M, Jia D, Jin T, Hou Y, Li R (2019) Dispersing mechanism and tribological performance of vegetable oil-based CNT nanofluids with different surfactants. Tribol Int 131:51–63. https://doi.org/10.1016/j.triboint.2018.10.025
20. Wang Y, Li C, Zhang Y, Li B, Yang M, Zhang X, Guo S, Liu G (2016) Experimental evaluation of the lubrication properties of the wheel/workpiece interface in MQL grinding with different nanofluids. Tribol Int 99:198–210. https://doi.org/10.1016/j.triboint.2016.03.023

21. Yang M, Li C, Zhang Y, Jia D, Li R, Hou Y, Cao H, Wang J (2019) Predictive model for minimum chip thickness and size effect in single diamond grain grinding of zirconia ceramics under different lubricating conditions. Ceram Int 45(12):14908–14920. https://doi.org/10.1016/j.ceramint.2019.04.226

22. Jia D, Zhang Y, Li C, Yang M, Gao T, Said Z, Sharma S (2022) Lubrication-enhanced mechanisms of titanium alloy grinding using lecithin biolubricant. Tribol Int 169:107461. https://doi.org/10.1016/j.triboint.2022.107461

23. Li H, Zhang Y, Li C, Zhou Z, Nie X, Chen Y, Cao H, Liu Bo, Zhang N, Said Z, Debnath S, Jamil M, Ali HM, Sharma S (2022) Cutting fluid corrosion inhibitors from inorganic to organic: progress and applications. Korean J Chem Eng. https://doi.org/10.1007/s11814-021-1057-0

24. Sulgani MT, Karimipour A (2019) Improve the thermal conductivity of 10w40-engine oil at various temperature by addition of Al2O3/Fe2O3 nanoparticles. J Mol Liq 283:660–666

25. Faulkner D, Khotan M, Shekarriz R (2003) Practical design of a 1000 W/cm/sup 2/cooling system [High Power Electronics]. In Ninteenth Annual IEEE Semiconductor Thermal Measurement and Management Symposium, 2003. (pp. 223–230). IEEE.

26. Wu S, Zhu D, Li X, Li H, Lei J (2009) Thermal energy storage behavior of Al2O3–H2O nanofluids. Thermochim Acta 483(1–2):73–77

27. Hosseini M, Ghader S (2010) A model for temperature and particle volume fraction effect on nanofluid viscosity. J Mol Liq 153(2–3):139–145

28. Soltani O, Akbari M (2016) Effects of temperature and particles concentration on the dynamic viscosity of MgO-MWCNT/ethylene glycol hybrid nanofluid: experimental study. Physica E 84:564–570

29. Ruhani B, Toghraie D, Hekmatifar M, Hadian M (2019) Statistical investigation for developing a new model for rheological behavior of ZnO–Ag (50%–50%)/Water hybrid Newtonian nanofluid using experimental data. Physica A 525:741–751

30. Esfe MH, Raki HR, Emami MRS, Afrand M (2019) Viscosity and rheological properties of antifreeze based nanofluid containing hybrid nano-powders of MWCNTs and TiO2 under different temperature conditions. Powder Technol 342:808–816

31. Esfe MH, Esfandeh S, Arani AAA (2019) Proposing a modified engine oil to reduce cold engine start damages and increase safety in high temperature operating conditions. Powder Technol 355:251–263

32. Esfe MH, Rostamian H, Sarlak MR (2018) A novel study on rheological behavior of ZnO-MWCNT/10w40 nanofluid for automotive engines. J Mol Liq 254:406–413

33. Alidoust S, AmoozadKhalili F, Hamedi S (2022) Investigation of effective parameters on relative thermal conductivity of SWCNT (15%)-Fe3O4 (85%)/water hybrid ferro-nanofluid and presenting a new correlation with response surface methodology. Colloids Surf, A 645:128625

34. Bindu MV, Joselin Herbert GM (2022) Thermal conductivity and viscosity of Al2O3-ZnO-MWCNT-EG ternary nanofluid. Int J Energy Res 46:17478

35. Chu YM, Ibrahim M, Saeed T, Berrouk AS, Algehyne EA, Kalbasi R (2021) Examining rheological behavior of MWCNT-TiO2/5W40 hybrid nanofluid based on experiments and RSM/ANN modeling. J Mol Liq 333:115969

36. Esfe MH, Abad ATK, Fouladi M (2019) Effect of suspending optimized ratio of nano-additives MWCNT-Al2O3 on viscosity behavior of 5W50. J Mol Liq 285:572–585

37. Tu J, Fan F, Qi C, Ding Z, Liang L (2022) Experimental study on the particle fouling properties of magnetic nanofluids in a corrugated tube with built-in twisted turbulator under variable magnetic field. Powder Technol 400:117216

38. Wang Y, Qi C, Zhao R, Wang C (2022) Study on the mechanism of modified surface and magnetic nanofluids on cooling performance of wireless charging equipment under magnetic field. Appl Therm Eng 208:118258

39. Tu J, Qi C, Li K, Tang Z (2022) Numerical analysis of flow and heat characteristic around micro-ribbed tube in heat exchanger system. Powder Technol 395:562–583

40. Tang Z, Qi C, Tian Z, Chen L (2022) Thermal management of electronic components based on new wave bio-inspired structures and nanofluids. Int Commun Heat Mass Transfer 131:105840

41. Tu J, Qi C, Tang Z, Tian Z, Chen L (2022) Experimental study on the influence of bionic channel structure and nanofluids on power generation characteristics of waste heat utilisation equipment. Appl Therm Eng 202:117893